Biogerontology
https://doi.org/10.1007/s10522-023-10043-0

RESEARCH ARTICLE

Identification of resibufogenin, a component of toad venom, as a novel senolytic compound in vitro and for potential skin rejuvenation in male mice

Kento Takaya · Toru Asou · Kazuo Kishi

Received: 9 May 2023 / Accepted: 29 May 2023

Abstract Senescent cells that accumulate with age have been shown to contribute to age-related diseases and organ dysfunction and have attracted attention as a target for anti-aging therapy. In particular, the use of senescent cell-depleting agents, or senolytics, has been shown to improve the aging phenotype in animal models. Since senescence has been implicated in the skin, particularly in fibroblasts, this study used aged human skin fibroblasts to investigate the effects of resibufogenin. A component of the traditional Chinese medicine toad venom, resibufogenin was investigated for senolytic and/or senomorphic activity. We found that the compound selectively caused senescent cell death without affecting proliferating cells, with a marked effect on the suppression of the senescence-associated secretory phenotype. We also found that resibufogenin causes senescent cell death by inducing a caspase-3-mediated apoptotic program. Administration of resibufogenin to aging mice resulted in an increase in dermal collagen density and subcutaneous fat, improving the phenotype of aging skin. In other words, resibufogenin ameliorates skin aging through selective induction of senescent cell apoptosis without affecting non-aged cells. This traditional compound may have potential therapeutic benefits in skin aging characterized by senescent cell accumulation.

Keywords Resibufogenin · Senotherapy · Senolytics · Aging phenotype · Fibroblast

Introduction

Senescent cells that have undergone repeated division show irreversible replicative arrest, a phenomenon first described as "cellular senescence" (Hayflick and Moorhead 1961). These cells, which have permanently stopped dividing, secrete a series of biologically active molecules, including inflammatory cytokines, growth factors, and matrix metalloproteinases: a characteristic known as the senescence-associated secretory phenotype (SASP) (Mamun et al. 2022; Janson et al. 2012). Senescent cell accumulation in aging tissues promotes premature aging and age-related diseases, such as chronic inflammation, liver fibrosis, atherosclerosis, insulin resistance, neurodegenerative diseases, and cancer (Tominaga 2015). In skin aging, SASP is caused by aging fibroblasts that accumulate in the epidermis, dermis, and subcutaneous adipose tissue (Velarde and Demaria 2016). The aging dermal layer contains an abundant extracellular matrix, composed of collagen and elastin, which contributes

K. Takaya · T. Asou · K. Kishi
Department of Plastic and Reconstructive Surgery, Keio University School of Medicine, Tokyo, Japan

K. Takaya (✉)
Keio University School of Medicine, 35 Shinanomachi, Shinjuku-ku, Tokyo 160-8582, Japan
e-mail: kentotakaya@keio.jp

Published online: 03 July 2023

to skin elasticity and maintains surface morphology. Abnormal extracellular matrix metabolism by senescent cells is one cause of skin aging, as the amount of matrix decreases with age, leading to loss of skin elasticity, delayed wound healing, and changes in surface morphology (Ezure et al. 2009; Xia et al. 2015).

Therefore, senescent cell removal is a major focus in the anti-aging treatment of systemic organs, including the skin. Genetic mouse model studies, in which senescent cells were selectively removed, revealed that senescent cell accumulation in aged tissues promotes senescence-associated decline and disease (Baker at al. 2016). Furthermore, in animal models, the removal of senescent cells by cell-removing chemical agents or genetic approaches improves healthy life expectancy and delays the development of aging phenotypes associated with functional impairment (Roos et al. 2016; Xu et al. 2018).

To date, a few anti-aging compounds have been identified and their senescent cell elimination properties validated, including navitoclax (Chang et al. 2016), dasatinib and quercetin (D + Q) (Saccon et al. 2021), and bis-2-(5-phenylacetamido-1,2,4-thiadiazol-2-yl)ethyl sulfide (BPTES) (Johmura et al. 2021). However, the safety of these newly developed agents has not been established, and serious side effects have been reported (Sharma et al. 2020; Al-Asmakh et al. 2021).

One solution is identifying new anti-aging effects of pre-existing drugs, as they already have suitable safety profiles. For example, metformin, an antidiabetic drug, has anti-aging effects as well as affecting insulin resistance (Papanagnou et al. 2022). Thus, we focused on drug repositioning. We hypothesized that drugs with known anti-inflammatory effects may contain active compounds with senolytic and/or senomorphic properties. Therefore, we aimed to investigate the effects of resibufogenin (RBG) on senescent cells. RBG is a traditional natural medicine originating from frog poison, widely used in China, with reported cardiotonic, analgesic effects, and antitumor effects (Xie et al. 2000; Wei et al. 2019). Although its specific anticancer activity and mechanism of action are unknown, one theory suggests that it induces apoptosis in a caspase-dependent manner or through G1 phase arrest (Wang et al. 2010; Ichikawa et al. 2015). As an underlying mechanism, RBG also induces PKC-dependent inhibition of GSK-3 activation. Subsequently, this decreases growth factor β-activated kinase 1 (TAK1) levels and suppression of IκB kinase activity via suppression of constitutive nuclear factor-κB (NF-κB) activity and its target gene expression (Liu et al. 2018). Alternatively, regulation of the MAPK/ERK signaling pathway and production of reactive oxygen species have also been noted (Takaya et al. 2022, 2023).

Thus, in this study, we hypothesized that the effects of RBG on senescent cells would be similar to the effect on cancer cells. We investigated the selective apoptosis-inducing effect of RBG on aging dermal fibroblasts and subsequently evaluated its efficacy on aging skin in vivo.

Methods

The study protocol was reviewed and approved by the Institutional Animal Care and Use Committee of the Keio University School of Medicine [Approval Number: 13072-(2)]. All experiments were performed in accordance with the institutional guidelines on animal experimentation.

Cell culture

Normal human dermal fibroblasts (NHDF; C-12,300) were obtained from PromoCell GmbH (Heidelberg, Germany). The PromoCell strain was isolated from a 24-year-old (NHDF-c24, lot: 4081903.2) donor, gender unknown. Repetitive senescence (RS) was determined as a cell population doubling level of 40 or greater and no cell proliferation for more than 2 weeks, according to previous studies (Kamiya et al. 2021). For ionizing radiation-induced senescence, cells were irradiated with 10 Gy of X-rays using the AB-160 X-ray irradiation system (AcroBio, Tokyo, Japan) and observed 10 days later. Control (proliferating) cells were mock-irradiated; this involved removal from the incubator, transportation to the irradiator, and maintenance outside the irradiator for the same period as the irradiated cells. To confirm the arrest of cell division, cells were treated with the BrdUFlowEx FITC Kit (EXBIO Praha, a.s., Vestec, Czech Republic) and flow cytometer (BD Bio-sciences, Franklin

Lakes, NJ, USA), and processed and analyzed using FlowJo (version 10.2) according to the manufacturer's protocol.

Senescence-associated β-galactosidase assay

Senescence-associated β-galactosidase (SA-βGal) activity in senescence-induced fibroblasts was assessed using the Senescence β-Galactosidase Staining Kit from Cell Signaling Technology (Danvers, MA, USA) according to the manufacturer's protocol. Briefly, the growth medium was aspirated from the 24-well plate, the wells were washed once with phosphate-buffered saline (PBS), 250 µL of fixative solution (1X) was added to each well, and the plate was incubated at room temperature (20–25 °C) for 10 min. The solution was removed, the wells were washed twice with PBS, and 250 µL of 1X SA-βGal detection solution was added before incubation overnight in the dark at 37 °C. The detection solution was aspirated, washed once with PBS, and bright-field images were taken using an upright microscope (NIKON ECLIPSE Ci-L; Nikon Instruments Inc, Melville, NY, USA), then PBS was added again.

Cell viability assay

Senescent or normal human skin fibroblasts were plated in 96-well plates (5×10^3 cells/well, n = 3) and maintained in 100 µL of medium. After 24 h, RBG (FUJIFILM Wako Pure Chemical Co., Osaka, Japan) or ABT-263 (AdipoGen Life Sciences Inc., San Diego, CA, USA) was administered to the medium at indicated concentrations (0.1, 0.5, 1, 2.5, and 5 µmol/L). After 72 h of incubation, cell viability was analyzed using the CellTiter-Glo® 2.0 Cell Viability Assay (Promega, Madison, WI, USA). Relative viability was normalized to that of the dimethyl sulfoxide (DMSO) control, and quantification experiments were performed in triplicate.

Apoptosis assay

To confirm apoptosis of senescent cells, the cells were treated with RBG (5 µM) or ABT-263 (5 µM) for 72 h with concentrations and dosing timings determined from the results of the previous cell survival assay and previous literature (Wang et al. 2014). The cells were fixed with 4% paraformaldehyde and incubated for 1 h at 37 °C after staining, according to the manual of the MEBSTAIN Apoptosis terminal deoxynucleotidyl transferase biotin-dUTP nick end labeling (TUNEL) Kit Direct (MBL, Nagoya, Japan). Counterstaining was performed using propidium iodide (5 µg/mL).

RNA extraction and reverse transcription

Total RNA was extracted from cells and tissues using the RNeasy mini kit (Qiagen, Hilden, Germany) according to the manufacturer's instructions. Total RNA was mixed with random primers, reverse transcriptase, and deoxynucleotide mixture (Takara Bio). The mixture was incubated in a T100™ thermal cycler (Bio-Rad Laboratories, Inc., Hercules, CA, USA) at 25 °C for 5-min annealing, 55 °C for 10-min synthesis, and 80 °C for 10-min heat inactivation of reverse transcriptase to obtain cDNA.

Real-time quantitative polymerase chain reaction (RT-qPCR)

RT-qPCR was performed using the Applied Biosystems 7500 Fast Real-Time PCR System (Thermo Fisher Scientific). PCR was performed in two steps: holding reagents at 95 °C for 3 s (denaturation) and at 60 °C for 30 s (annealing and extension). A total of 40 cycles were performed and the fluorescence of each sample was measured at the end of each cycle. In the subsequent stage of melting curve analysis, the temperature was increased from 60 to 95 °C, and fluorescence was measured continuously. Gene expression was determined using primers for Il-6 (Hs00985639_m1), IL-1a (Hs00174092_m1), matrix metalloproteinase (MMP) 3 (Hs00968305_m1), MMP9 (Hs00957562_m1), and tumor necrosis factor (TNF)-α(Hs02621508_s1) (all Thermo Fisher Scientific); PCR master mix [Cat. GAPDH (Hs02786624_g1)] was used as a control gene sample for normalization. Gene expression levels in the proliferating cell population were used as baseline values, and fold change values were determined using the $2\text{-}\Delta\Delta C^T$ method.

Enzyme-linked immunosorbent assay (ELISA)

The senescent cell model was prepared as described above and the medium was changed to a serum-free medium containing antibiotics. After 24 h, the

conditioned medium was collected and analyzed using the following ELISA kits according to the manufacturer's protocol: Human IL-1α Quantikine ELISA Kit (DLA 50), Human IL-8 Quantikine ELISA Kit (D8000C), Human Total MMP-3 DuoSet ELISA (DY513), and Human MMP-9 DuoSet ELISA (DY911) (all from R&D Systems, Inc, Minneapolis, MS, USA).

Western blotting

Total protein was extracted from cells and tissues using RIPA buffer (FUJIFILM Wako Pure Chemical Co.) according to the manufacturer's protocol. Each sample (30 μg) was electrophoresed on 10% polyacrylamide gels (Mini-PROTEAN® TGX™ Precast Gels, Bio-Rad Laboratories, Inc, CA, USA) and transferred to a Trans-Blot Turbo Transfer System (Bio-Rad). After blocking with 3% fat-free milk at room temperature (20–25 °C) for 1 h, the cells were incubated overnight at 4 °C with the following primary antibodies diluted in blocking solution with shaking: p16 (ab108349, 1:200 dilution, Abcam), p21 (ab220206, 1:100 dilution, Abcam), Bcl-xL (1:200 dilution, Cell signaling), pro caspase-3 antibody (ab32150, 1:200 dilution, Abcam), cleaved caspase-3 antibody (ab32042, 1:100 dilution, Abcam), and glyceraldehyde 3-phosphate dehydrogenase (GAPDH 1:2000 dilution; Santa Cruz, Santa Cruz, CA, USA) washed three times with Tri Buffered Saline + Tween 20. Then, the slides were incubated with goat anti-rabbit IgG H&L (HRP) (ab205718; Abcam, 1:5000) for 1 h at 37 °C. After washing, the bands were treated with an electrochemiluminescence detection kit (Pierce Biotechnology, Rockford, IL, USA) for 3 min, and the chemiluminescence imager (ImageQuant LAS4000mini; GE Healthcare, Chicago, IL, USA) was used to obtain images of the bands. Image analysis was performed using ImageJ (Version 1.53p; NIH, Bethesda, MD, USA). Each experiment was repeated three times.

In vivo mouse assay

Male Institute of Cancer Research (ICR) mice (80–90 weeks, 20 ± 2 g, SPF) were obtained from Sankyo Laboratories (Tokyo, Japan). All procedures were performed according to the ARRIVE guidelines and approved by the Animal Ethics Committee of Keio University School of Medicine. Mice were kept under specific pathogen-free conditions with a constant 12-h light/dark cycle with free access to a standard diet and water. Anesthetic inhalation (isoflurane) and other necessary efforts were made to alleviate animal suffering in the study.

ICR mice were randomly divided into two groups (n = 4): a negative control group (vehicle) and an RBG group (10 mg/kg RBG). RBG was dissolved in saline containing DMSO (5%, v/v) and Tween-80 (2%, v/v); RBG concentrations and the administration protocol followed those used without adverse events in a previous study (Gao et al. 2022). After an overnight fast, mice were administered RBG intraperitoneally (ip), and negative controls received the same amount of vehicle. The mice were euthanized after receiving one dose each for 12 consecutive days. Dorsal skin was collected and analyzed. After overnight fixation in 4% PFA and embedding in paraffin, specimens were sliced into 7-μm-thick sections and stained with Masson trichrome (MT). To quantify collagen density, the background of MT images was subtracted (n = 3–5, at least three microscopic fields of view per group) and the color deconvolution plug-in of ImageJ software was used. Specifically, the RGB images were separated into three 8-bit background images of each color, and then the blue component was evaluated. A square region of interest (ROI) (0.01 mm^2) was randomly assigned to a subbasal area that did not contain skin appendages, and the density of integration was measured as the sum of pixel values within the ROI.

Immunohistochemistry

Paraffin-embedded specimens were sliced into 7-μM-thick slices, mounted on glass slides, and allowed to dry overnight. They were immersed in xylene for 3 min 5 times and hydrated with 100%, 90%, 80%, and 70% ethanol and milliQ water. To block nonspecific binding sites, slides were incubated with 2% goat serum in PBS for 1 h at room temperature (20–25 ℃). The slides were then incubated with the primary antibody p16ink4a (ab108349, Abcam, 1:200) overnight at 4 °C. After washing three times with PBS, the slides were incubated with a 1:1000

dilution of Alexa Fluor 488 conjugated goat anti-rabbit antibody (Thermo Fisher Scientific) in PBS for 1 h at room temperature (20–25 °C). After washing three times with PBS, ProLongGold anti-fading with 4′,6-diamidino-2-phenylindole (DAPI) Inclusion Medium (ThermoFisher Scientific) was used for nuclear contrast staining. The staining was performed using ProLong Gold anti-fading with 6-diamidino-2-phenylindole (DAPI) Inclusion Medium (ThermoFisher Scientific).

Statistical analysis

Statistical analyses were performed using the GraphPad Prism (version 5.0; San Diego, CA, USA) or SPSS 22.0 (Chicago, IL, USA) software. One-way analysis of variance and Tukey's post hoc test were used to compare differences between three or more groups. Statistical significance was set at $P < 0.05$.

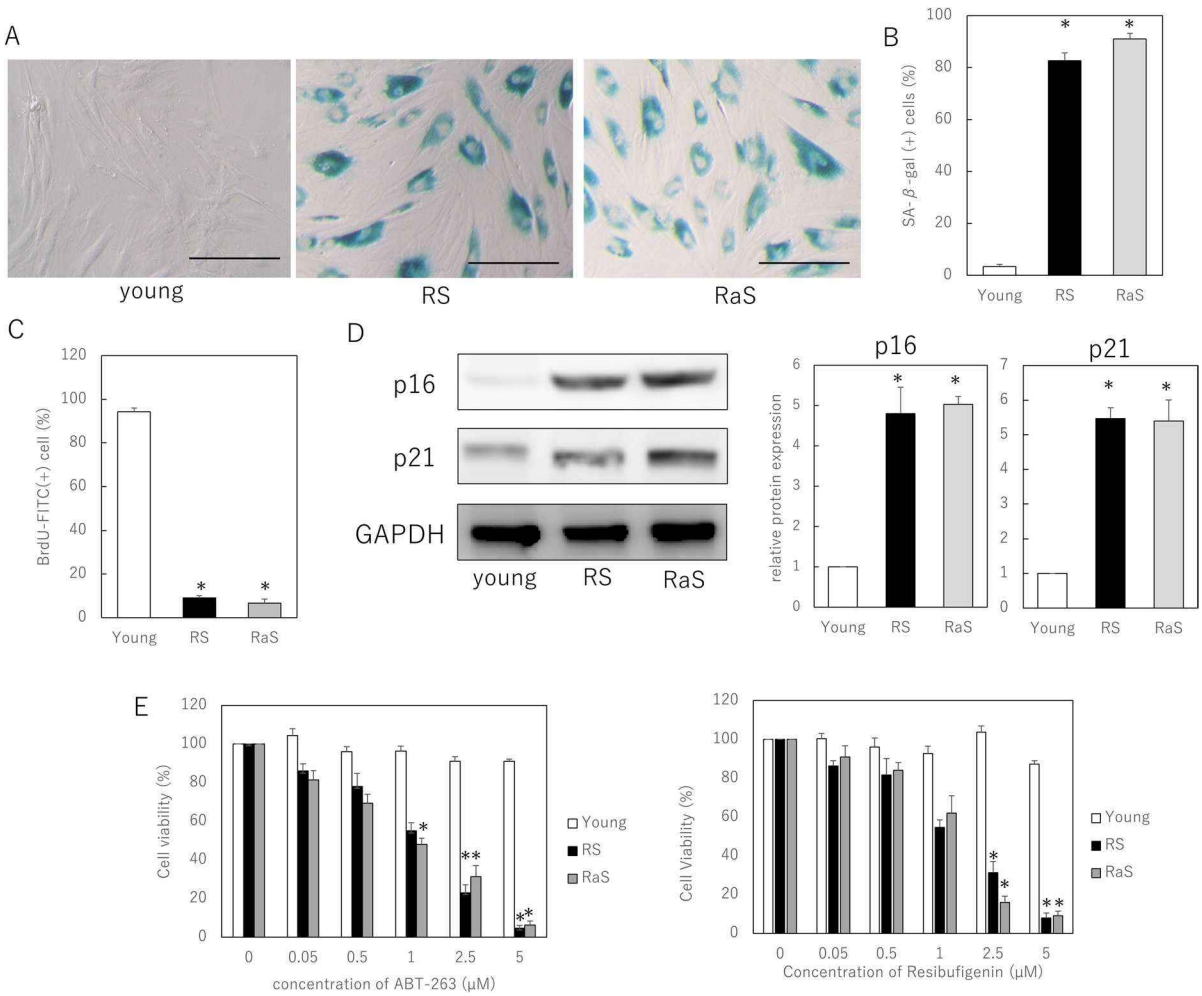

Fig. 1 Effects of anti-aging drugs on aging human skin fibroblasts. **A** SA-β-gal staining image. bar = 100 μm. **B** Percentage of SA-β-gal positive cells. **C** Percentage of BrdU-positive cells determined by flow cytometry. **D** Comparison of expression of senescence-associated proteins p16 and p21. **E** Effects of ABT-263 and resibufogenin on cell removal. After induction of cellular senescence, cells were treated with the indicated concentrations of each drug for 72 h (n = 4). Cell viability was measured to determine the effect of the senescent cell removal agents. All experiments were performed independently in triplicate. *$p < 0.05$. *RS* replicative senescence; *RaS* ionizing radiation-induced senescence

Results

RBG eliminates senescent cells

Initially, we induced senescence in human skin fibroblasts using replicative senescence (RS) and ionizing radiation-induced senescence (RaS). An increase in SA-β-gal positive cells (Fig. 1A, B) and a significant decrease in bromodeoxyuridine (BrdU) absorption (mitotic potential) (Fig. 1C) was observed. We also observed a significant increase in the expression of senescence-related proteins, such as p16 and p21, in these senescence-induced cells (Fig. 1D). The cytotoxic effect of RBG was compared to that of ABT-263, known to target senescent cells. After 48 h of treatment with 2.5 and 5 μM RBG, there was a significant reduction in the viability of two senescent cell types, with no effect on the viability of proliferating cells (Fig. 1E). The dose response curve showed a biphasic dose response: a typical closed curve.

RBG suppresses SASP

The effects of RBG on SASP-related cytokines and chemokines were tested. qRT-PCR revealed that SASP-related cytokines IL-1a, IL-6, and TNF-α, and mRNA expression of SASP molecules, including MMP-3 and MMP-9, were elevated in aging skin fibroblasts. This expression was not significantly altered in the control group, whereas treatment with RBG significantly decreased this expression in both treatment groups (Fig. 2A, B). ELISA also showed that the secreted levels of cytokines of IL-1a, IL-6, MMP3, and MMP9 were significantly decreased after RBG treatment (Fig. 2C, D).

RBG promotes apoptosis of senescent cells

To determine whether RBG affects the apoptotic pathway in the removal of senescent cells, we performed an apoptosis assay after RBG treatment. We found that, for young cells, RBG treatment did not increase the number of TUNEL-positive cells; however, in senescent cells, a large number of TUNEL-positive apoptotic cells were observed (Fig. 3A). To investigate RBG involvement in apoptosis in detail, we examined the levels of cleaved caspase-3 (apoptosis-promoting marker) and Bcl-XL (anti-apoptotic protein) in senescent cells treated with RBG. RBG induced increased cleaved caspase-3 levels, an apoptotic protein in senescent cells (Fig. 3B). These results indicate that RBG-induced senescent cell death is likely through caspase-3-dependent apoptosis.

Fig. 2 Effect of resibufogenin on SASP suppression. **A**, **B** Effect of resibufogenin on SASP genes. Relative mRNA levels of SASP-related genes as measured using RT-qPCR. Data were normalized against mRNA obtained from young cells; GAPDH was used as an endogenous control. **C**, **D** ELISA assay to determine the effect of resibufogenin on SASP proteins. Data are expressed as mean ± SEM. All experiments are performed independently in triplicate. *$p < 0.05$. *SASP* senescence-associated secretory phenotype; *RS* replicative senescence; *RaS* ionizing radiation-induced senescence; *RBG* resibufogenin

RBG treatment results in dermal collagen thickening and increased subcutaneous fat

To investigate the skin rejuvenating effects of RBG in vivo, RBG was administered intraperitoneally to older male ICR mice. Consequently, histologically, there was a statistically significant thickening of collagen fibers in the dermis and subcutaneous adipose tissue (Fig. 4A).

To observe the effect of RBG on the removal of senescent cells in the dermis, p16-positive cells were also observed. The results showed that RBG treatment significantly reduced p16-positive (senescent) cells (Fig. 4B).

Discussion

Senescent cells accumulation in the skin has gained much attention, as it is hypothesized to induce skin aging, via cell immortalization and accelerated fibrosis due to SASP. Senotherapy, including senolytics and/or senomorphics, selectively targets senescent cells to reduce their detrimental effects. In skin aging, the treatment of senescent fibroblasts with ABT-263 and BPTES, typical senolytic drugs, suppresses the aging phenotype (Kim et al. 2022). However, since the safety of these drugs is not yet understood, drug repositioning, to utilize the effects of existing drugs and senolytics, and developing new drugs are both important.

In this study, we focused on RBG, a component of toad venom that is a traditional natural medicine.

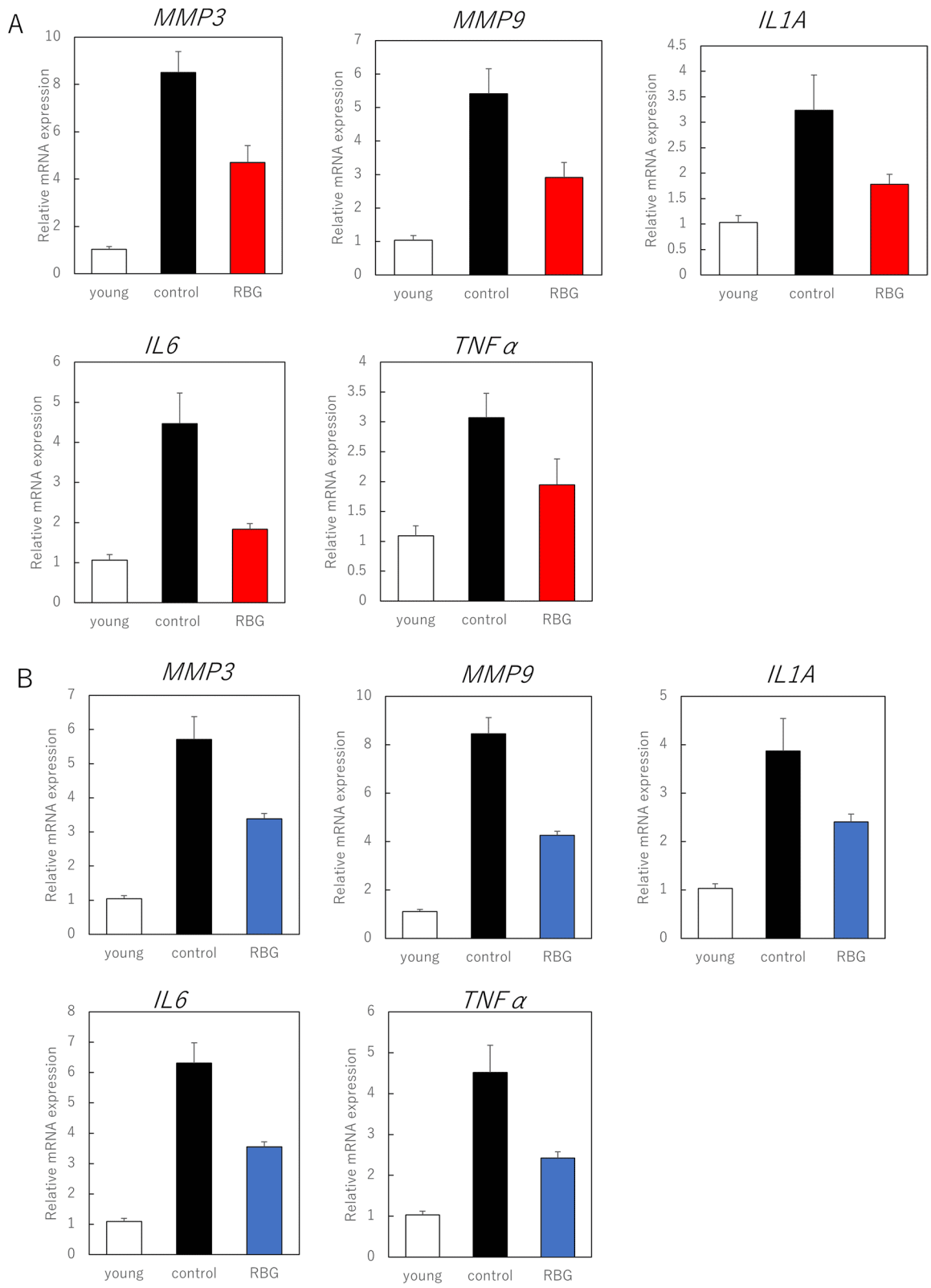
A
MMP3
MMP9
IL1A
IL6
TNFα
B
MMP3
MMP9
IL1A
IL6
TNFα
Relative mRNA expression
young
control
RBG

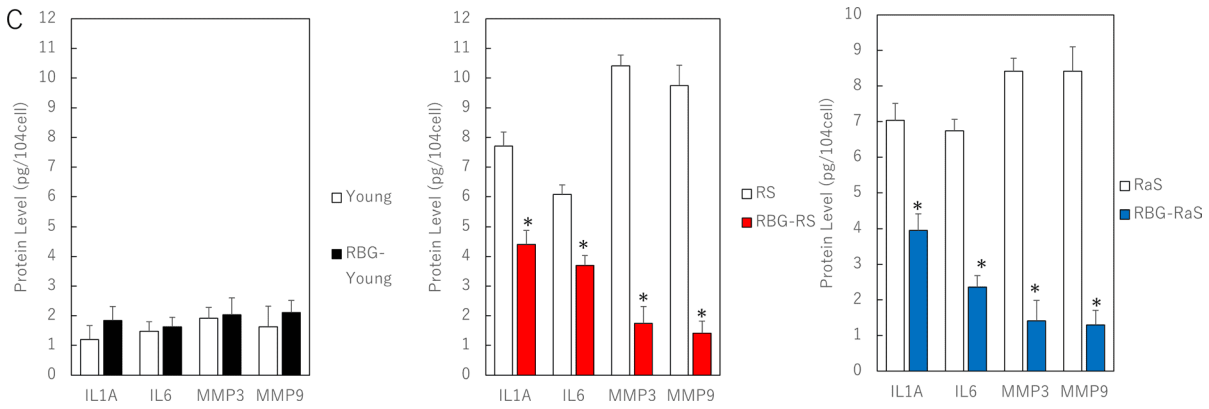

Fig. 2 (continued)

Toad venom has been used in China for hundreds of years to treat various diseases (Li et al. 2021a, b). Over the past decade, a growing number of studies have shown that toad venom components can be utilized in the development of potential cancer therapeutics. The primary antitumor mechanisms identified include induction of apoptosis or/and autophagy, cell cycle arrest, inhibition of cell metastasis, reversal of drug resistance, and inhibition of cancer cell growth. A recent study showed that RBG exerts anti-tumorigenic and anti-glycation effects in breast cancer via the inhibitory effect of miR-143-3p on hexokinase 2 expression, offering new therapeutic possibilities (Guo et al. 2022). Furthermore, RBG causes ferroptosis, mainly in a glutathione peroxidase 4 inactivation-dependent manner, thereby exerting antitumor activity (Lu et al. 2018). Therapeutic approaches to cancer share similarities with senotherapy as they specifically target abnormal cells; these findings support RBG application as a senolytic drug.

In this study, we found that RBG had both senolytic and senomorphic effects on senescent fibroblasts. Our findings showed that RBG induced caspase-3-mediated apoptosis in a senescent cell-specific manner. Previous studies have demonstrated that RBG effectively inhibited cell proliferation and induced apoptosis and caspase-3 and caspase-8 activity in MGC-803 cells, supporting our results (Coppe et al. 2010). However, while these results suggest that the anticancer effect of RBG induces gastric cancer cell death via the PI3K/AKT/GSK3β signaling pathway, our study did not show the involvement of these pathways (data not shown), suggesting further study is needed into the mechanism behind RBG-induced senescent cell apoptosis.

In addition, we observed inhibition of SASP, suppressing senescence. Activated SASPs include a variety of chemokines, inflammatory cytokines, growth factors, and matrix-restructuring enzymes that affect the microenvironment (Birch and Gil 2020), all of which were suppressed by RBG treatment. Furthermore, administration of RBG to aging mice reversed the aging phenotype by increasing collagen density in the dermis and increasing subcutaneous fat. This phenomenon, attributed to the reduction of p16-positive senescent cells within the dermis, suggested that RBG could be a potential anti-aging drug candidate in the context of geriatric medicine.

Moreover, hormetin, which uses a potential toxin to produce biologically beneficial effects through activating one or more stress response pathway (Calabrese et al. 2019), may explain the anti-aging effects of resibufogenin. Constituents of some medicinal plants used in traditional Chinese medicine and Indian Ayurvedic medicine are claimed to have hormesis-induced anti-aging effects (Rattan and Clark 1994). For example, sertasterol and peoniflorin have cytoprotective effects and induce synthesis of heat shock proteins (HSP) in human cells (Westerheide et al. 2004). Ashwagandha (*Withania somnifera*) leaf extract also induces HSP synthesis in mammalian cells. Increased HSP levels, the main activator of hormesis, may prevent protein denaturation; increased proteasome activity in cells treated with mild heat shock is involved in the removal of damaged proteins (Beedholm et al. 2004; Rattan 2005). The heat shock-induced hormesis

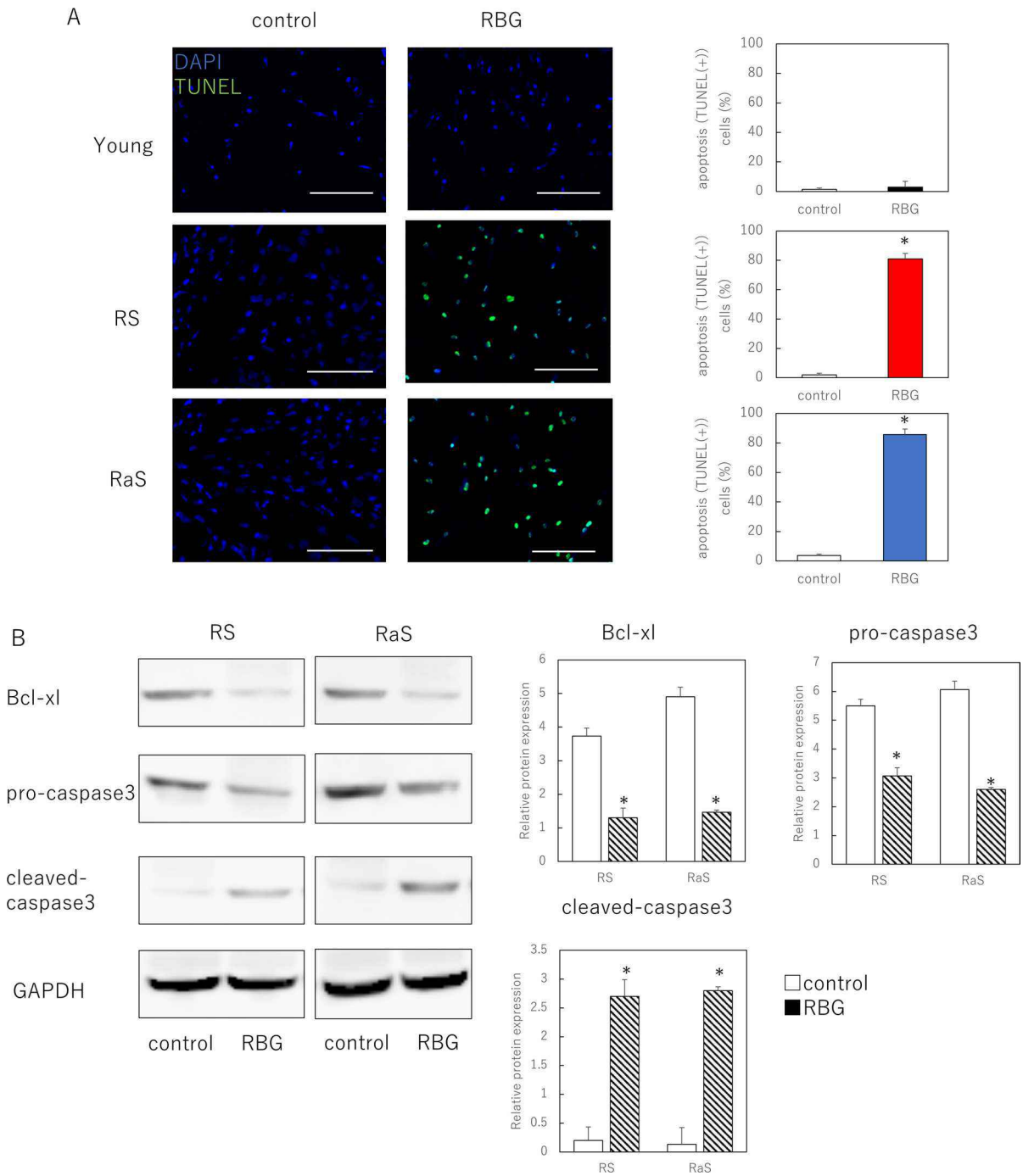

Fig. 3 Resibufogenin induces apoptosis specifically in senescent cells. **A** Observation of apoptosis by TUNEL assay. Bar = 100 µm. **B** Comparison of expression of proteins associated with apoptosis. GAPDH was used as endogenous control. All experiments are performed independently in triplicate. *p < 0.05. *SASP* senescence-associated secretory phenotype; *RS* replicative senescence; *RaS* ionizing radiation-induced senescence; *RBG* resibufogenin

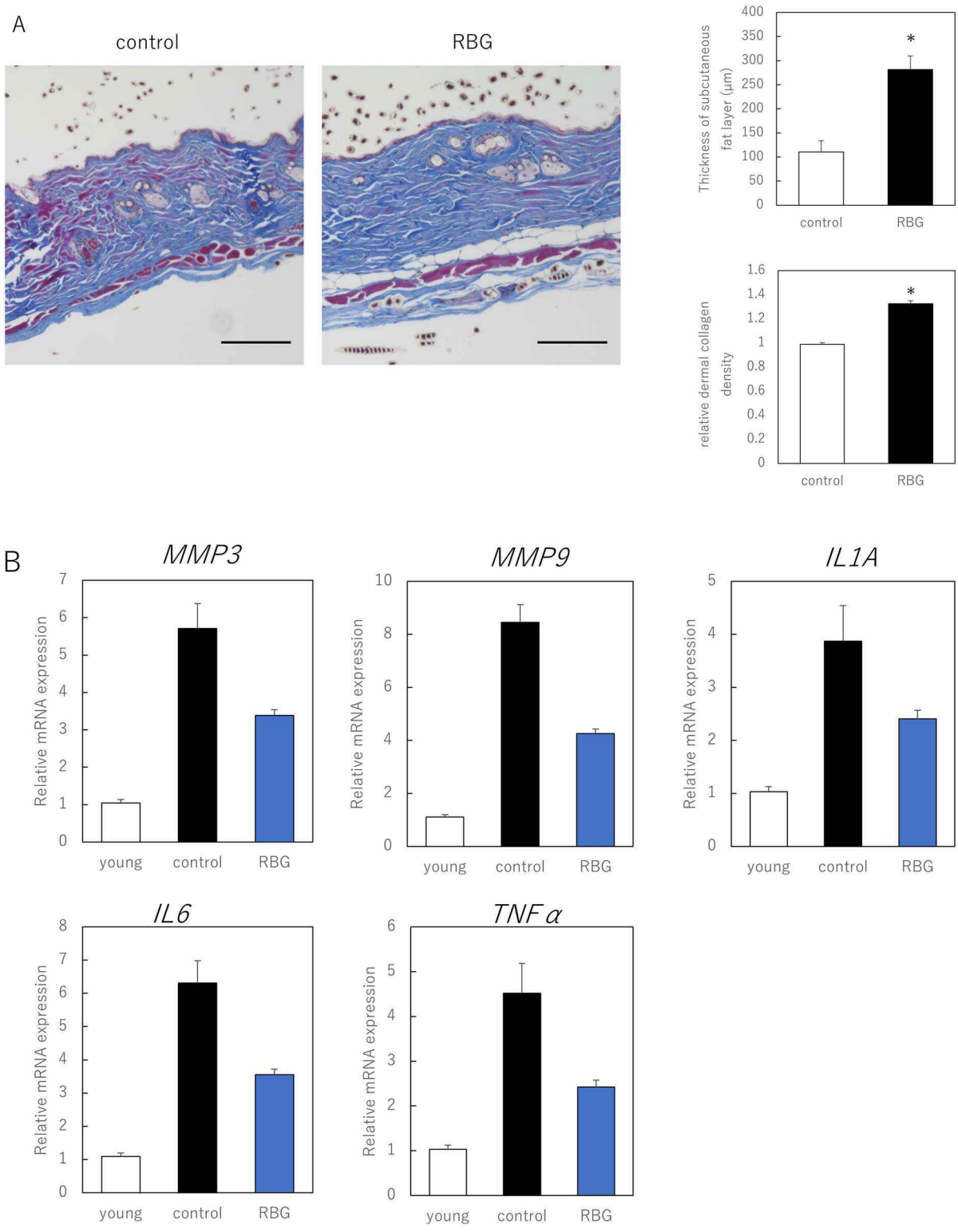

Fig. 4 Resibufogenin improves the skin phenotype of aging mice. **A** Comparison of histological images by Masson Trichrome staining. Bar = 200 μm. **B** Immunofluorescence staining of p16 positive cells. bar = 100 μm. *p < 0.05. *RBG* resibufogenin

effect on senescence is accompanied by stress kinase activation and increased Na-K-ATPase sodium pump activity (Nielsen et al. 2006). Therefore, future investigation of the hormesis effect of RBG via these mechanisms may help to explain the anti-aging effect on skin discovered in this study.

The anti-aging effects of RBG observed in our study indicate its role in the regulation of inflammation and the immune system; we identified its novel senolytic/senomorphic properties via apoptosis by caspase-3 in this study. Additional investigations are needed to fully characterize the mechanisms of its senolytic/senomorphic effects. Although fibroblasts, the most abundant cells in the dermis, were targeted in this study, the effects of RBG on other skin component cells, such as keratinocytes, follicular system cells, and macrophages, are not clear. Furthermore, since only male mice were used in this study to avoid hormonal effects, additional experiments are needed to examine the effects on female mice. In addition, further studies are needed to investigate the effects on other organs, side effects of administration, in vivo anti-aging activity, and the effects of long-term course of RBG administration.

Conclusion

The selective clearance of senescent dermal fibroblasts and inhibition of SASP by RBG were demonstrated in this study. Thus, this compound may provide an effective option for treating skin aging due to senescent fibroblast accumulation.

Acknowledgements The authors would like to thank all laboratory staff for their technical assistance with the experiments. The authors declare no conflicts of interest. The funders had no role in the study design, collection, analyses, or interpretation of data, writing of the manuscript, or decision to publish the results.

Author contributions Conceptualization, KT and TA; methodology, KT and KK; software, KT; validation, KT, TA, and KK.; formal Analysis, KT; investigation, KT; resources, KK; data curation, KT; writing—original draft preparation, KT; writing—review & editing, TA and KK; visualization, KT; supervision, TA and KK; project administration, KK; funding acquisition, KK.

Funding This work was supported by the Japan Society for the Promotion of Science, KAKENHI program, grant number JP 22K19589.

Data availability The data presented in this study are available upon request from the corresponding author.

Declarations

Competing interests The authors declare no competing interests.

Experiments involving human and/or animal participants All animal procedures were performed according to the ARRIVE guidelines and approved by the Animal Ethics Committee of Keio University School of Medicine.

References

Al-Asmakh M, Bawadi H, Hamdan M, Gupta I, Kheraldine H, Jabeen A, Rizeq B, Al Moustafa AE (2021) Dasatinib and PD-L1 inhibitors provoke toxicity and inhibit angiogenesis in the embryo. Biomed Pharmacother 134:111134

Baker DJ, Childs BG, Durik M, Wijers ME, Sieben CJ, Zhong J, Saltness RA, Jeganathan KB, Verzosa GC, Pezeshki A, Khazaie K, Miller JD, van Deursen JM (2016) Naturally occurring p16(Ink4a)-positive cells shorten healthy lifespan. Nature 530:184–189

Beedholm R, Clark BFC, Rattan SIS (2004) Mild heat stress stimulates proteasome and its 11S activator in human fibroblasts undergoing aging in vitro. Cell Stress Chaperones 9:49–57

Birch J, Gil J (2020) Senescence and the SASP: many therapeutic avenues. Genes Dev 34:1565–1576

Calabrese EJ, Agathokleous E, Kapoor R, Kozumbo WJ, Rattan SIS (2019) Re-analysis of herbal extracts data reveals that inflammatory processes are mediated by hormetic mechanisms. Chem Biol Interact 314:108844

Chang J, Wang Y, Shao L et al (2016) Clearance of senescent cells by ABT263 rejuvenates aged hematopoietic stem cells in mice. Nat Med 22:78–83

Coppé J-P, Desprez P-Y, Krtolica A, Campisi J (2010) The senescence-associated secretory phenotype: the dark side of tumor suppression. Annu Rev Pathol 5:99–118

Ezure T, Hosoi J, Amano S, Tsuchiya T (2009) Sagging of the cheek is related to skin elasticity, fat mass and mimetic muscle function. Skin Res Technol 15:299–305

Gao Y, Xu Z, Li X, Liu Z, Li W, Kang Y, Zhang X, Qi Y (2022) Resibufogenin, one of bufadienolides in toad venom, suppresses LPS-induced inflammation via inhibiting NF-κB and AP-1 pathways. Int Immunopharmacol 113:109312

Guo Y, Liang F, Zhao F, Zhao J (2022) Retraction note: resibufogenin suppresses tumor growth and Warburg effect through regulating miR-143-3p/HK2 axis in breast cancer. Mol Cell Biochem 477:2687

Hayflick L, Moorhead PS (1961) The serial cultivation of human diploid cell strains. Exp Cell Res 25:585–621

Ichikawa M, Sowa Y, Iizumi Y, Aono Y, Sakai T (2015) Resibufogenin induces G1-Phase arrest through the proteasomal degradation of cyclin D1 in human malignant tumor cells. PLoS ONE 10:e0129851

Janson DG, Saintigny G, van Adrichem A, Mahé C, El Ghalbzouri A (2012) Different gene expression patterns in

human papillary and reticular fibroblasts. J Invest Dermatol 132:2565–2572
Johmura Y, Yamanaka T, Omori S, Wang TW, Sugiura Y, Matsumoto M, Suzuki N, Kumamoto S, Yamaguchi K, Hatakeyama S, Takami T, Yamaguchi R, Shimizu E et al (2021) Senolysis by glutaminolysis inhibition ameliorates various age-associated disorders. Science 371:265–270
Kamiya Y, Odama M, Mizuguti A, Murakami S, Ito T (2021) Puerarin blocks the aging phenotype in human dermal fibroblasts. PLoS ONE 22:16:e0249367
Kim H, Jang J, Song MJ, Kim G, Park CH, Lee DH, Lee SH, Chung JH (2022) Attenuation of intrinsic ageing of the skin via elimination of senescent dermal fibroblasts with senolytic drugs. J Eur Acad Dermatol Venereol 36:1125–1135
Li H, Liu L, Huang T, Jin M, Zheng Z, Zhang H, Ye M, Liu K (2021a) Establishment of a novel ferroptosis-related lncRNA pair prognostic model in colon adenocarcinoma. Aging 13:23072–23095
Li FJ, Hu JH, Ren X, Zhou CM, Liu Q, Zhang YQ (2021b) Toad venom: a comprehensive review of chemical constituents, anticancer activities, and mechanisms. Arch Pharm 354:e2100060
Liu L, Liu Y, Liu X, Zhang N, Mao G, Zeng Q, Yin M, Song D, Deng H (2018) Resibufogenin suppresses transforming growth factor-β-activated kinase 1-mediated nuclear factor-κB activity through protein kinase C-dependent inhibition of glycogen synthase kinase 3. Cancer Sci 109:3611–3622
Lu Z, Xu A, Yuan X, Chen K, Wang L, Guo T (2018) Anticancer effect of resibufogenin on gastric carcinoma cells through the phosphoinositide 3-kinase/protein kinase B/glycogen synthase kinase 3β signaling pathway. Oncol Lett 16:3297–3302
Mamun AA, Sufian MA, Uddin MS, Sumsuzzman DM, Jeandet P, Islam MS, Zhang HJ, Kong AN, Sarwar MS (2022) Exploring the role of senescence inducers and senotherapeutics as targets for anticancer natural products. Eur J Pharmacol 928:174991
Nielsen ER, Eskildsen-Helmond Y, Rattan SIS (2006) MAP-kinases and heat shock-induced horme-sis in human fibroblasts during serial passaging in vitro. Ann NY Acad Sci U S A 1067:343–348
Papanagnou ED, Gumeni S, Sklirou AD, Rafeletou A, Terpos E, Keklikoglou K, Kastritis E, Stamatelopoulos K, Sykiotis GP, Dimopoulos MA, Trougakos IP (2022) Autophagy activation can partially rescue proteasome dysfunction-mediated cardiac toxicity. Aging Cell 21:e13715
Rattan SIS (2005) Hormetic modulation of aging and longevity by mild heat stress. Dose-response 3:533–546
Rattan SIS, Clark BF (1994) Kinetin delays the onset of ageing characteristics in human fibroblasts. Biochem Biophys Res Commun 201:665–672
Roos CM, Zhang B, Palmer AK, Ogrodnik MB, Pirtskhalava T, Thalji NM, Hagler M, Jurk D, Smith LA, Casaclang-Verzosa G, Zhu Y, Schafer MJ, Tchkonia T et al (2016) Chronic senolytic treatment alleviates established vasomotor dysfunction in aged or atherosclerotic mice. Aging Cell 15:973–977
Saccon TD, Nagpal R, Yadav H, Cavalcante MB, Nunes ADC, Schneider A, Gesing A, Hughes B, Yousefzadeh M, Tchkonia T, Kirkland JL, Niedernhofer LJ, Robbins PD et al (2021) Senolytic Combination of Dasatinib and Quercetin alleviates intestinal senescence and inflammation and modulates the gut microbiome in aged mice. J Gerontol A Biol Sci Med Sci 76:1895–1905
Sharma AK, Roberts RL, Benson RD Jr, Pierce JL, Yu K, Hamrick MW, McGee-Lawrence ME (2020) The Senolytic Drug Navitoclax (ABT-263) causes trabecular bone loss and impaired osteoprogenitor function in aged mice. Front Cell Dev Biol 8:354
Takaya K, Ishii T, Asou T, Kishi K (2022) Glutaminase inhibitors rejuvenate human skin via clearance of senescent cells: a study using a mouse/human chimeric model. Aging 14:8914–8926
Takaya K, Ishii T, Asou T, Kishi K (2023) Navitoclax (ABT-263) rejuvenates human skin by eliminating senescent dermal fibroblasts in a mouse/human chimeric model. Rejuvenation Res In Press 26:9–20
Tominaga K (2015) The emerging role of senescent cells in tissue homeostasis and pathophysiology. Pathobiol Aging Age Relat Dis 5:27743
Velarde MC, Demaria M (2016) Targeting senescent cells: possible implications for delaying skin aging: a Mini-Review. Gerontology 62:513–518
Wang DL, Qi FH, Xu HL, Inagaki Y, Orihara Y, Sekimizu K, Kokudo N, Wang FS, Tang W (2010) Apoptosis-inducing activity of compounds screened and characterized from cinobufacini by bioassay-guided isolation. Mol Med Rep 3:717–722
Wang ZJ, Sun L, Heinbockel T (2014) Resibufogenin and cinobufagin activate central neurons through an ouabain-like action. PLoS ONE 9:e113272
Wei WL, An YL, Li ZW, Wang YY, Ji HJ, Hou JJ, Wu WY, Guo DA (2019) Simultaneous determination of resibufogenin and its eight metabolites in rat plasma by LC-MS/MS for metabolic profiles and pharmacokinetic study. Phytomedicine 60:152971
Westerheide SD, Bosman JD, Mbadugha BNA et al (2004) Celastrols as inducers of the heat shock response and cytoprotection. J Biol Chem 279:56053–56060
Xia W, Quan T, Hammerberg C, Voorhees JJ, Fisher GJ (2015) A mouse model of skin aging: fragmentation of dermal collagen fibrils and reduced fibroblast spreading due to expression of human matrix metalloproteinase-1. J Dermatol Sci 78:79–82
Xie JT, Wang H, Attele AS, Yuan CS (2000) Effects of resibufogenin from toad venom on isolated Purkinje fibers. Am J Chin Med 28:187–196
Xu M, Pirtskhalava T, Farr JN, Weigand BM, Palmer AK, Weivoda MM, Inman CL, Ogrodnik MB, Hachfeld CM, Fraser DG, Onken JL, Johnson KO, Verzosa GC et al (2018) Senolytics improve physical function and increase lifespan in old age. Nat Med 24:1246–1256